Transplantation of Human Placenta-Derived Multipotent Stem Cells Reduces Ischemic Brain Injury in Adult Rats

Kou-Jen Wu,* Seong-Jin Yu,* Chia-Wen Chiang,† Kuna-Hung Cho,‡ Yu-Wei Lee,§
B. Linju Yen,§ Li-Wei Kuo,† and Yun Wang*

*Center for Neuropsychiatric Research, National Health Research Institutes (NHRI), Miaoli, Taiwan
†Institute of Biomedical Engineering and Nanomedicine, NHRI, Miaoli, Taiwan
‡Institute of Brain Science, National Yang-Ming University, Taipei, Taiwan
§Regenerative Medicine Research Group, Institute of Cellular and System Medicine, NHRI, Miaoli, Taiwan

After the onset of stroke, a series of progressive and degenerative reactions, including inflammation, are activated, which leads to cell death. We recently reported that human placenta-derived multipotent stem cells (hPDMCs) process potent anti-inflammatory effects. In this study, we examined the protective effect of hPDMC transplants in a rodent model of stroke. Adult male Sprague–Dawley rats were anesthetized. hPDMCs labeled with a vital dye of fluorescing microparticles, DiI, or vehicle were transplanted into three cortical areas adjacent to the right middle cerebral artery (MCA). Five minutes after grafting, the right MCA was transiently occluded for 60 min. Stroke animals receiving hPDMCs showed a significant behavioral improvement and reduction in lesion volume examined by T2-weighted images 4 days poststroke. Brain tissues were collected 1 day later. Human-specific marker HuNu immunoreactivity and DiI fluorescence were found at the hPDMC graft sites suggesting the survival of hPDMCs in host brain. Grafting of hPDMCs suppressed IBA-1 immunoreactivity and deramification of IBA-1⁺ cells in the perilesioned area, suggesting activation of microglia was attenuated by the transplants. Taken together, our data indicate that hPDMC transplantation reduced cortical lesions and behavioral deficits in adult stroke rats, and these cells could serve as a unique anti-inflammatory reservoir for the treatment of ischemic brain injury.

Key words: Ischemia; Placenta; Stem cells; Transplantation; Inflammation

INTRODUCTION

Stroke is the third leading cause of death and the most common cause of adult disability worldwide. Tissue plasminogen activator is the only FDA-approved pharmacological treatment for acute ischemic stroke. However, this treatment has to be initiated within 3 to 4 h after onset of stroke. Seeking other effective treatments with much wider therapeutic time windows is critically important.

After the onset of stroke, a series of progressive and degenerative reactions, including inflammation, are activated, which lead to cell death and affect neurorepair (32). Stroke-induced inflammation can extend for days after injury (25). It is thus likely that treatment aiming at inflammatory therapy may have relatively long-lasting therapeutic effects. Stroke-mediated inflammation involves two sources: (a) innate inflammation, which involves activation of microglia, overproduction and release of cytokines and chemokines in brain, and disruption of the blood–brain barrier (BBB) in brain. Stroke also exacerbates (b) adaptive

inflammation including infiltration of peripheral immune cells through the ruptured BBB [see review by Lee et al. (18)]. The release of proinflammatory molecules from these immune cells contributes to neurodegeneration (11). A number of anti-inflammatory chemical or cell therapies have been examined in acute stroke animals and patients. For example, daily treatment with minocycline reduced morphological activation of microglia in areas adjacent to the infarction in stroke animals (38). Similarly, intravenous transplantation of human embryonic neural stem cells (H1 clone) during the acute stage attenuated peripheral inflammatory responses and inflammatory infiltration into the brain after hemorrhagic stroke (17). These anti-inflammatory therapies have been shown to reduce cerebral infarction and neurological deficits.

Placental cells are easily isolated with less ethical concern. We previously isolated multipotent stem cells from human term placenta (36). These human placenta-derived multipotent stem cells (hPDMCs) exhibit embryonic stem

cell surface markers of stage-specific embryonic antigen 4, TRA-1-61, and TRA-1-80. After culturing under the appropriate conditions, hPDMCs can differentiate to adipogenic, osteogenic, chondrogenic, and neurogenic cells (35,36). In addition to their multilineage differentiation capacity, hPDMCs have been shown to possess strong and unique immunomodulatory effects (8). Similar to bone marrow mesenchymal stromal cells (BMMSCs), hPDMCs suppress allogeneic effector T-lymphocyte functions, while increasing the number of regulatory T-lymphocytes, a population of immunomodulatory lymphocytes. Moreover, the presence of interferon- (IFN-), a proinflammatory cytokine, enhances the immunosuppressive properties of hPDMCs (8). hPDMCs enhance immunomodulatory leukocytes of the innate immune system, increasing the number of myeloid-derived suppressor cells and modulating monocytes into an immunosuppressive phenotype (10,33). Furthermore, hPDMCs, but not BMMSCs, upregulated the immunomodulatory molecule human leukocyte antigen (HLA)-G upon exposure to IFN- and reduced natural killer lymphocyte (NK)/interleukin (IL)-2-mediated apoptosis (21). Moreover, we have recently demonstrated the therapeutic utility of hPDMCs in ischemic heart disease, using both a small animal (mouse) model as well as a large animal (pig) model of acute myocardial infarction (unpublished observation). With these anti-highly immunomodulatory and multipotent properties, hPDMCs may be useful for protection and regeneration in an ischemic brain disease such as stroke.

The present study is aimed to investigate the influence of hPDMCs on functional outcome, infarct volume, and inflammation in stroke rats. Our data support that hPDMC transplantation reduced cortical lesions and behavioral deficits in adult stroke rats, and these cells could serve as a unique anti-inflammatory reservoir for the treatment of ischemic brain injury.

MATERIALS AND METHODS

Isolation, Expansion, and Labeling of hPDMCs

Term (38–40 weeks' gestation) placentas (two males and one female) from healthy donor mothers were obtained with informed consent and approved by the Institutional Review Board of the National Health Research Institutes, Taiwan. The hPDMCs were isolated as previously reported (36). Cell cultures were maintained at 37°C with a water-saturated atmosphere and 5% CO_2. Medium was replaced one to two times every week. hPDMCs were labeled with the fluorescent dye chloromethylbenzamido 1,1 -dioctadecyl-3,3,3 3 -tetramethylindocarbocyanine perchlorate (CM-DiI; Gibco-Invitrogen, Grand Island, NY, USA) prior to injection into rats as described previously (31). In brief, cells (4×10^5) were labeled with 2.5 ∝l/ml of CM-DiI for 10 min, washed with PBS and centrifuged. Cells were resuspended in culture medium at 5×10^4 cells/∝l.

Animals and Surgery

Twenty-eight adult male Sprague–Dawley rats (BioLASCO, Taipei, Taiwan), weighing 250–300 g, were used in this study. Seventeen animals were given a stroke as described, while 11 acted as control (nonstroke) animals. The use of animals was approved by the Animal Care and Use Committee, National Health Research Institutes. Animals were anesthetized with chloral hydrate (0.4 g/kg, IP, Sigma-Aldrich). A craniotomy was performed to expose the right middle cerebral artery (MCA). PDMCs were prepared immediately prior to transplantation as described above and then loaded into a 25-∝l Hamilton syringe (Reno, NV, USA). hPDMCs were transplanted into three cortical areas adjacent to the bifurcation of right MCA. The approximate coordinates for these sites were 1.0–2.0 mm anterior to the bregma and 3.5–4.0 mm lateral to the midline; 0.5–1.5 mm posterior to the bregma and 4.0–4.5 mm lateral to the midline; and 4.0–4.5 mm posterior to the bregma and 5.5–6.0 mm lateral to the midline. Five microliters of hPDMCs (5×10^4 viable cells/∝l; $n = 7$) or vehicle (culture media; $n = 10$) was injected at 1 ∝l/min into each site using an Ultra MicroPumpII (World Precision Instruments, Sarasota, FL, USA). The needle was retained in place for 5 min after each transplantation.

Approximately 10 min after the last injection of cells, animals were subjected to cerebral ischemia. The right distal MCA was occluded by 10-0 suture (N-2540, Monosof™ Covidien, Minneapolis, MN, USA) for 60 min as previously described (23,24). Core body temperature wasmonitored and maintained at 37°C with a heating pad during surgery. After surgery, the animals were kept in a temperature-controlled incubator to maintain body temperature at 37°C. After recovery from the anesthesia, the animals were returned to their home cages.

Behavioral Measurement

Two behavioral tests were used to analyze stroke behavior as previously described. (a) Body asymmetry was analyzed using an elevated body swing test (6,7). (b) Neurological deficits were evaluated by the Bederson's test (5).

Magnetic Resonance Imaging (MRI)

MRI experiment was performed on a 7T animal scanner (Biospec 70/30 AS, Bruker Biospin MRI, Ettlingen, Germany) with an actively shielded gradient (BGA-12-S, 670 mT/m, 175-ms rise time). A linear volume resonator was used for RF pulse transmission, and an actively decoupled surface coil was used for RF signal reception. The rats were anesthetized with isoflurane (Baxter, Taipei, Taiwan; 3% induction and 1% maintenance in 30% O_2/70% N_2) and secured in a custom-made animal holder with a dedicated water heated rat bed, maintaining the rat body temperature at 37°C. To assure the same placement within the magnet

from scan to scan, each rat was fixed in the same position by using inbuilt earplugs, tooth bar, and nose mask. A pressure sensor (SA Instruments, Inc., Stony Brook, NY, USA) was positioned under the abdomen of the rat to monitor respiration (maintained at 45 55 breaths/min).

T2-weighted images (T2WI) and diffusion tensor imaging (DTI) data were acquired on each rat on day 4 poststroke. A fast spin-echo sequence, rapid acquisition with refocused echoes, was employed to acquire the T2WI and localize the desired slice positions. The sequence parameters of T2WI were repetition time (TR) of 2,742 ms, echo time (TE) of 33 ms, slice thickness of 1 mm, 25 slices, matrix size of 256×256, number of excitations (NEX) of 4, and field of view (FOV) of 25×25 mm^2. The DTI data was acquired with a four-shot spin-echo diffusion-weighted echo planar imaging (DWI) sequence incorporating with 12 diffusion-encoding gradient directions. The diffusion sensitivity (b-value) was 1,000 s/mm^2 and one unweighted DWI (b-value = 0 s/mm^2) was acquired. The sequence parameters of DWI are TR of 6,250 ms, TE of 21 ms, diffusion time ( ) of 13 ms, diffusion gradient pulse duration ( ) of 3 ms, FOV of 25×25 mm^2, slice thickness of 1 mm, 25 slices (identical slice positions as T2WI), matrix size of 128×128, and NEX of 2. The total scan time was approximately 30 min.

MRI Data Analysis

For T2WI analysis, the regions of interest (ROIs) defining the infarction areas were identified on a high-resolution T2WI with in-plane resolution of 100×100 ∝m^2. ROIs were manually determined by two of the authors (CWC and LWK) to enclose the hyperintensity regions in T2WI after contrast adjustment. Lesion volume (LV) was calculated by the summation of total volume within ROIs from all lesion-contaminating T2-weighted image slices.

For DTI analysis, diffusion tensors were reconstructed by using an in-house program written in Matlab (The Mathworks, Natick, MA, USA). Two indices, fractional anisotropy (FA) and apparent diffusion coefficient (ADC), were computed from the diffusion tensor by conventional DTI model (3). For each voxel, the diffusion tensor is diagonalized to derive three eigenvalues ($_1$, $_2$, and $_3$) corresponding to three eigenvectors ($_1$, $_2$, and $_3$) (3,4). Mean ADC value of each voxel is defined as the average of those three eigenvalues, reflecting the water molecular displacement in a given diffusion time. To quantify the tissue directional integrity, FA of each voxel is defined as

$$FA = \sqrt{\frac{3}{2}} \frac{\sqrt{(_1 - _M)^2 + (_2 - _M)^2 + (_3 - _M)^2}}{\sqrt{_1^2 + _2^2 + _3^2}}$$

Where $_M = (_1 + _2 + _3)/3$.

The ROIs used for DTI analysis were identified on FA and ADC with in-plane resolution of 200×200 ∝m^2. For FA analysis, the ROIs were applied on white matter (external capsules) of both lesioned and the corresponding contralateral sides around the slice located at bregma. Besides, mean ADC was assessed by selecting ROIs on the infarction (lesioned cortex) region using the same slice. An additional ROI was placed in the mirror region in the contralateral side for comparison. All ROIs were manually determined by two of the authors (CWC and LWK) for DTI analysis.

Hematoxylin and Eosin (H&E) and IBA1 Immunostaining

Stroke rats receiving hPDMCs or vehicle transplantation were perfused intracardially with 4% paraformaldehyde (Sigma-Aldrich; 100 ml/min) in 0.1 M phosphate buffer (PB;Sigma-Aldrich), pH 7.3. Brains were removed from the skull, postfixed for 18–20 h at 4°C, rinsed with PB and sequentially transferred to 10%, 20%, and 30% sucrose solutions. Brains were then frozen on dry ice and sectioned on a cryostat to obtain coronal sections 30 μm in thickness.

H&E staining: Brain sections were mounted on gelatin-coated slides and dried. Hematoxylin QS (H-3404; Vector Laboratories, Burlingame, CA, USA) was applied to each slide for 1 min at room temperature. After washing of slides, slides were incubated with 1% eosin Y solution (Vector Laboratories) for 1 min. Slides were washed again and then covered using cytoseal™ 60 (Thermo Scientific, Waltham, MA, USA). The area of infarction was quantified and averaged in three consecutive brain sections with a visualized anterior commissure per each animal.

Immunostaining: Brain sections were rinsed in PB and were blocked with 4% bovine serum albumin (Sigma-Aldrich) with 0.3% Triton X-100 (Sigma-Aldrich) in 0.1 mol/L PB. Sections were then incubated with monoclonal anti-ionized calcium-binding adapter molecule 1 (IBA1; 1:100, Chemicon, Billerica, MA, USA) or human antinuclear antibody (HuNu, 1:100, Millipore, Billerica, MA, USA) at 4°C overnight. Sections were rinsed in 0.1 mol/L PB and incubated in Alexa Fluor 488 secondary antibody solution (1:500; Molecular Probes, Eugene, OR, USA); nuclei were stained with 1 ∝g/ml 4,6-diamidino-2-phenylindole (DAPI, Sigma-Aldrich). Control sections were incubated without primary antibody. Brain sections were mounted on slides and coverslipped. Confocal analysis was performed using a Nikon D-ECLIPSE 80i microscope (Melville, NY, USA) and EZ-C1 3.90 software as previously described (40).The optical density of IBA1 immunoreactivity and DiI fluorescence was quantified in three consecutive brain sections with a visualized anterior commissure in each animal. Ten photomicrograms were taken along the perilesioned region per brain slices; IBA1 optical density was analyzed by NIS Elements AR 3.2 Software

(Nikon) and was averaged in each brain for statistical analysis. All immunohistochemical measurements were done by blinded observers.

Statistics

Values are means ± SEM. Unpaired *t*-test, two-way ANOVA, and post hoc Newman–Keuls test were used for statistical analysis (Sigmaplot software ver. 12.5, San Jose, USA). A statistically significant difference was defined as $p < 0.05$.

RESULTS

Behavioral Improvement

A total of 17 rats were used for behavioral analysis. Animals were pretreated with vehicle ($n = 10$) or hPDMCs ($n = 7$) prior to stroke. Previous studies have shown that MCA ligation and reperfusion induce body asymmetry in experimental animals. In the elevated body asymmetry test taken on days 3 and 5 poststroke, we found that the frequency of swinging the body or head contralateral to the ischemic side was significantly higher in the stroke rats injected with vehicle than in those grafted with hPDMCs ($F_{1,30} = 9,887$, $p = 0.004$ two-way ANOVA) (Fig. 1A). Post hoc Newman–Keuls test indicated grafting of PDMCs significantly attenuated body asymmetry in the stroke at day 5 poststroke ($p = 0.004$).

Bederson's neurological test was carried out on days 3 and 5 after MCAo and sham surgery. In all nonstroke rats ($n = 11$), no neurological deficit was found, and Bederson's score was zero. In stroke animals ($n = 17$), transplantation of hPDMCs, compared to the vehicle, significantly reduced Bederson's score ($F_{1,30} = 4.515$, $p = 0.042$ two-way ANOVA) (Fig. 1B).

Localization of PDMC Transplant in the Lesioned Cortex

Fifteen rats (seven receiving hPDMCs and eight receiving vehicle) were used for immunohistological exam. hPDMCs were labeled with CM-DiI fluorescence prior to transplantation (Fig. 2A). Animals were perfused on day 5 after transplantation and stroke surgery. As seen in the representative photomicrograph in Figure 2B, CM-DiI (red) fluorescence in the PDMCs was confined to the graft sites in the cerebral cortex. No migration of grafted cells into adjacent cortical areas was seen. No red fluorescence was found in animals receiving vehicle (Fig. 2C).

The graft cells were also examined by immunohistochemistry. Human-specific marker HuNu (Fig. 2D) was identified in the grafted site only in animals receiving PDMCs. No HuNu immunoreactivity was found in the animals receiving vehicle. Most of CM-DiI⁺ cells (Fig. 2E) colabeled with HuNu (Fig. 2F). However, some HuNu⁺ cells did not contain CM-DiI fluorescence (Fig. 2F).
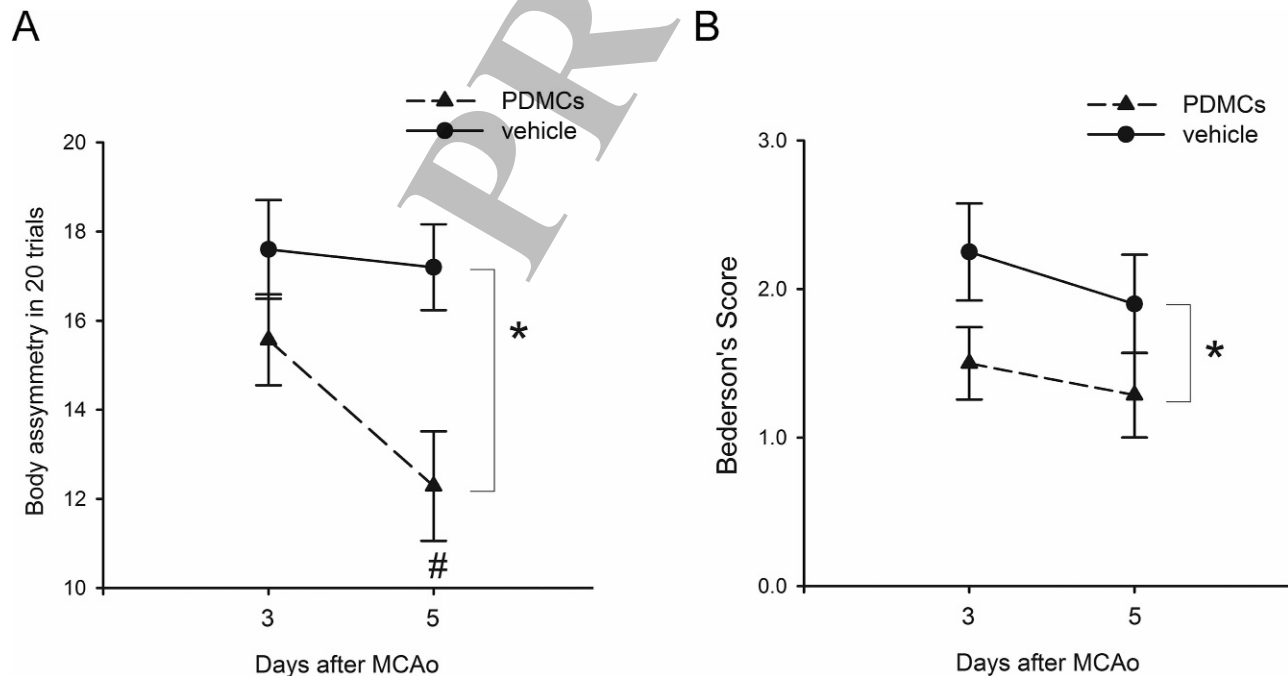
Figure 1. Transplantation of hPDMCs reduced behavioral deficits in stroke rats. (A) Animals receiving vehicle demonstrated close to 90% body asymmetry in 20 trials at 3 and 5 days after MCAo. Transplantation of hPDMCs significantly reduced body asymmetry on day 5 post-MCAo ($p < 0.001$). (B) Bederson's neurological tests were carried out on days 3 and 5 after treatment. Intracortical transplantation of hPDMCs significantly reduced Bederson's score ($p < 0.001$, two-way ANOVA).
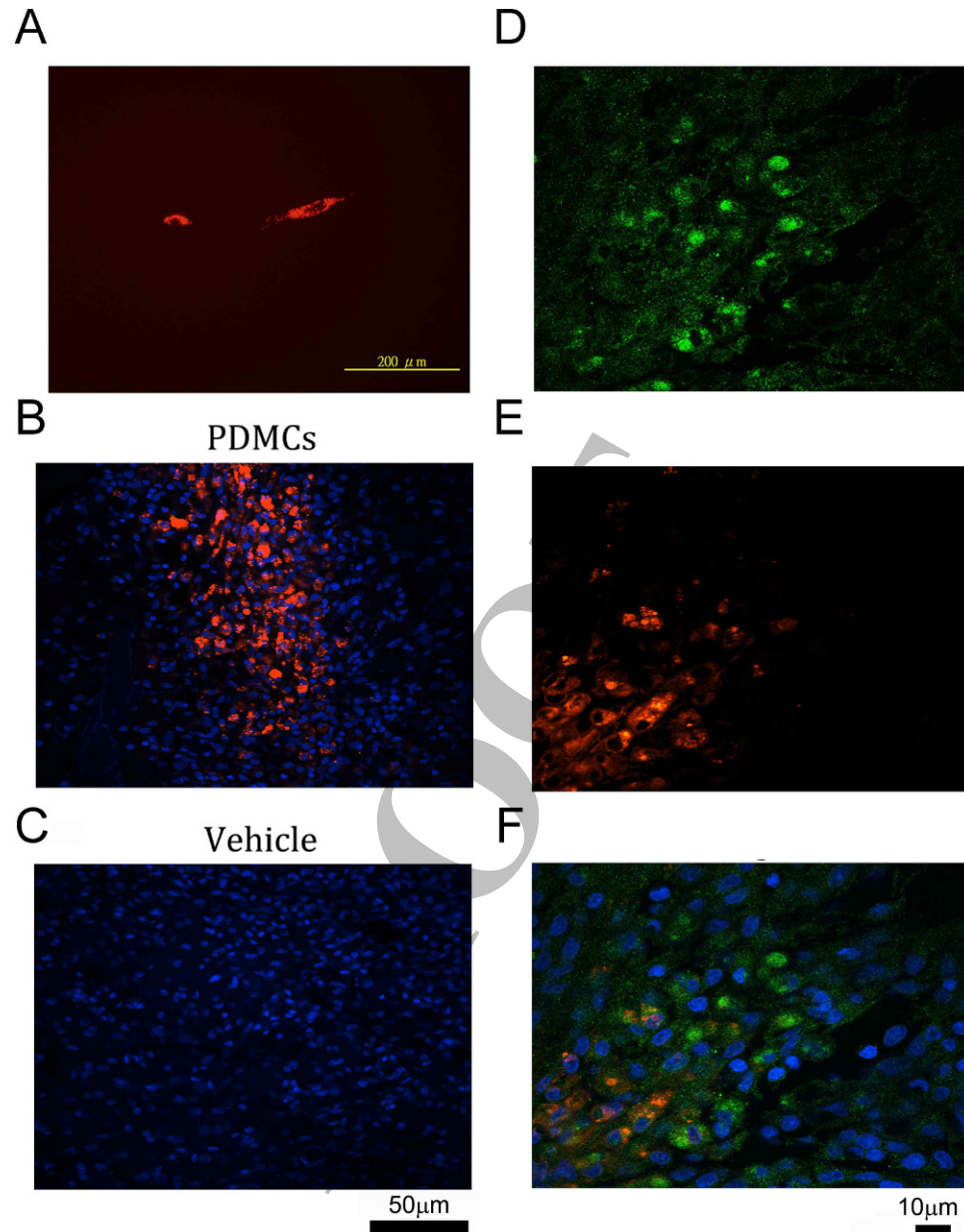
Figure 2. Localization of hPDMCs in host brain. (A) hPDMCs were prelabeled with fluorescent dye CM-DiI prior to grafting to stroke rats. Animals receiving PDMCs or vehicle were perfused on day 5 after transplantation and stroke surgery. (B) Red CM-DiI fluorescence⁺ cells were confined to the graft sites in cerebral cortex. (C) No red fluorescence was found in an animal receiving vehicle. (D) HuNu immunoreactivity (green) was found in the hPDMC-grafted site in another animal. (E) CM-DiI red fluorescence was also found in the same hPDMC graft site. (F) Merged photomicrograph (from D and E + DAPI) indicates that most of the CM-DiI⁺ cells colabeled with HuNu. Some HuNu⁺ cells did not contain CM-DiI fluorescence. (C, E, F) DAPI in blue color. Calibration: A: 200 ∝m, B, C: 50 ∝m, D, E, F: 10 ∝m

Brain Infarction

MRI experiments were performed on 16 stroke rats (seven receiving hPDMCs and nine receiving vehicle). The size of the lesion (infarction) was examined using T2WI acquired on day 4 after MCAo (Fig. 3). An increase in signal intensity of T2WI was found in the cortex of the lesioned side. LV was significantly reduced in hPDMC rats (91.6 ± 18.2 mm^3), compared to those receiving vehicle (141.7 ± 14.2 mm^3, $p = 0.04$, *t*-test) (Fig. 3C). Typical T2WIs from one animal treated with hPDMCs and vehicle are shown in Figure 3A1 and A2, respectively.

The size of brain infarction was also examined by H&E staining on day 5 poststroke in 15 stroke rats (seven receiving hPDMCs and eight receiving vehicle). MCA
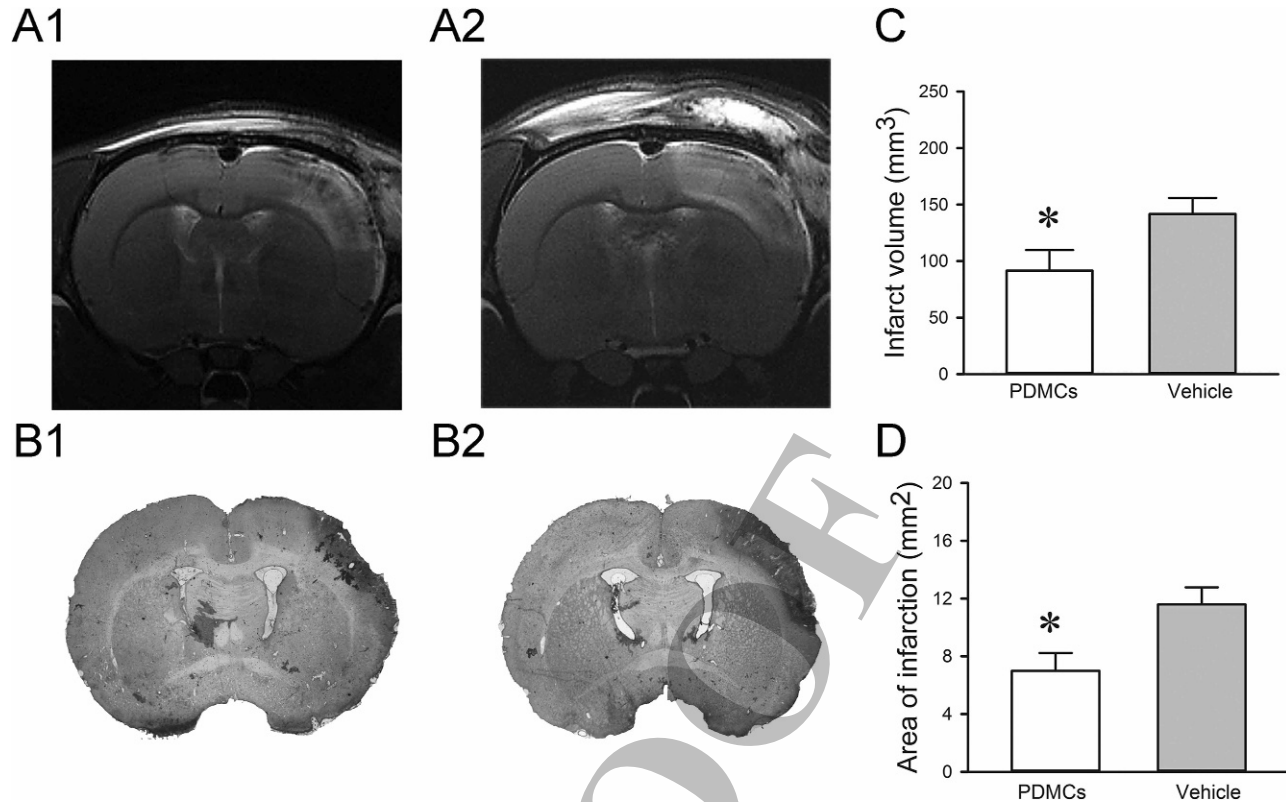
Figure 3. Transplantation of hPDMCs reduced cerebral infarction in stroke rats. (A) Representing T2WI taken at day 4 after MCAo indicates that the size of the lesion was reduced in animal-grafted hPDMCs (A1), compared to the other animal treated with vehicle (A2). Averaged infarct volume was significantly reduced by hPDMC graft (C, *$p < 0.05$). (B) Representative H&E images indicate that transplantation of PDMCs reduced brain infarction at 5 days after stroke (B1: hPDMCs vs. B2: vehicle). The largest infarction area per brain slice was significantly reduced by hPDMC graft (D, *$p = 0.0186$).

ligation and reperfusion resulted in clear-cut infarction of the lesioned side cortex in all the vehicle control animals studied, as seen in the representative H&E photomicrograph taken at the level of anterior commissure (Fig. 3B2). Transplantation of hPDMCs greatly reduced brain infarction (Fig. 3B1). The averaged largest infarction area per brain slice in each rat was significantly reduced by PDMC graft ($p = 0.0186$, t-test) (Fig. 3D).

DTI

A total of 16 stroke rats (seven receiving hPDMCs and nine receiving vehicle) were examined by DTI. Using a two-way ANOVA, we found a significant reduction in FA in the external capsule of the lesioned side compared to that of the contralateral side on day 4 after stroke in both hPDMCs and vehicle-treated groups ($p < 0.001$, $F_{1,28} = 16.891$). No difference in FA was seen between hPDMCs and vehicle-treated groups in the external capsule of the contralateral side ($p = 0.970$, post hoc Newman–Keuls test). FA ratio (rFA) was calculated by normalizing the FA values in the external capsule of the lesioned side to the corresponding value of the contralateral side. As shown

in Figure 4A3, no difference in rFA was seen between hPDMCs and vehicle-treated groups ($p = 0.986$, t-test). Typical FA maps from animals receiving hPDMC graft and vehicle are shown in Figure 4A1 and A2, respectively.

DTI-derived mean ADC values of lesion significantly increased in both hPDMCs and vehicle-treated rats compared with that of respective contralateral region ($p < 0.001$, $F_{1,28} = 146.214$, two-way ANOVA) (Fig. 4B1: hPDMCs, Fig. 4B2: vehicle). ADC values (rADC) in the cortex of the lesioned side were normalized to the corresponding value in the contralateral cortex. hPDMCs significantly increased rADC in the cortex of the lesioned side ($p < 0.001$; t-test) (Fig. 4B3).

PDMC Grafting Reduced Microglial Activation

Activation of microglia and inflammation in stroke brain has been well documented. Using the selective microglia marker IBA1, we found that the density of IBA1 immunoreactivity was greatly increased in the core (Fig. 5A) and perilesioned area (Fig. 6B) in the ischemic cortex, compared to the corresponding sites in the nonlesioned side cortex (Figs. 5D and 6C). High-magnification images
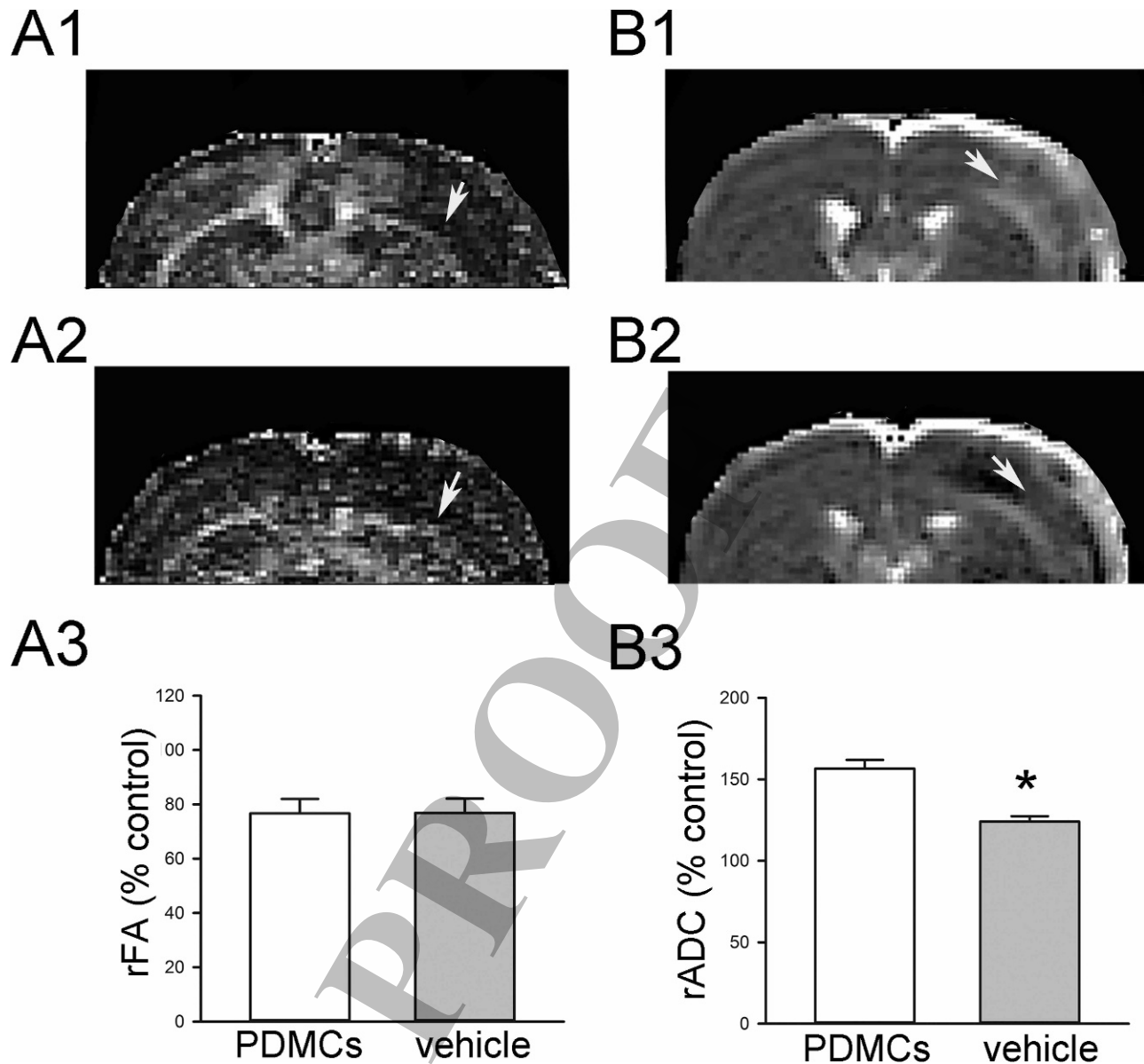
Figure 4. Stroke and hPDMC transplantation-mediated changes in FA and ADC. (A) FA was taken on day 4 after stroke in rats grafted with (A1) PDMCs or (A2) vehicle. (A3) FA values in the lesioned cortex were normalized (rFA) to the corresponding value in the contralateral white matter. Ischemic lesion significantly reduced rFA (A1, A2, arrows) in animals receiving hPDMCs or vehicle. No difference in rFA was seen between these two groups. (B) Representative ADC images in rats receiving (B1) hPDMCs and (B2) vehicle. (B3) hPDMCs significantly increased relative ADC (rADC) in the lesioned cortex (*$p < 0.001$).

indicated that resting microglia exhibited ramified morphology in the nonlesioned side cortex (Figs. 5D and 6C, insert), while deramified or ameboid microglial cells were found in the lesion core (Fig. 5A, insert) or perilesioned area (Fig. 6B, insert) in animals receiving vehicle. Transplantation of hPDMCs did not alter IBA1 immunoreactivity in regions away from the transplant in the lesioned core (Fig. 5B, insert); however, it partially reduced IBA1 activation inthe area adjacent (<300 ∝m) to the graft

(Fig. 5C, insert). In contrast, PDMCs greatly reduced microglia activation in the perilesioned area (Fig. 6A vs. B). PDMC transplantation reduced the IBA1 immunoreactivity as well as morphological activation of microglia in the perilesioned area. Ramified microglia were found in the perilesioned area in animals receiving PDMCs (Fig. 6, inserts). Averaged IBA1 optical density in the perilesioned zone was significantly reduced by PDMC transplantation (Fig. 6D).
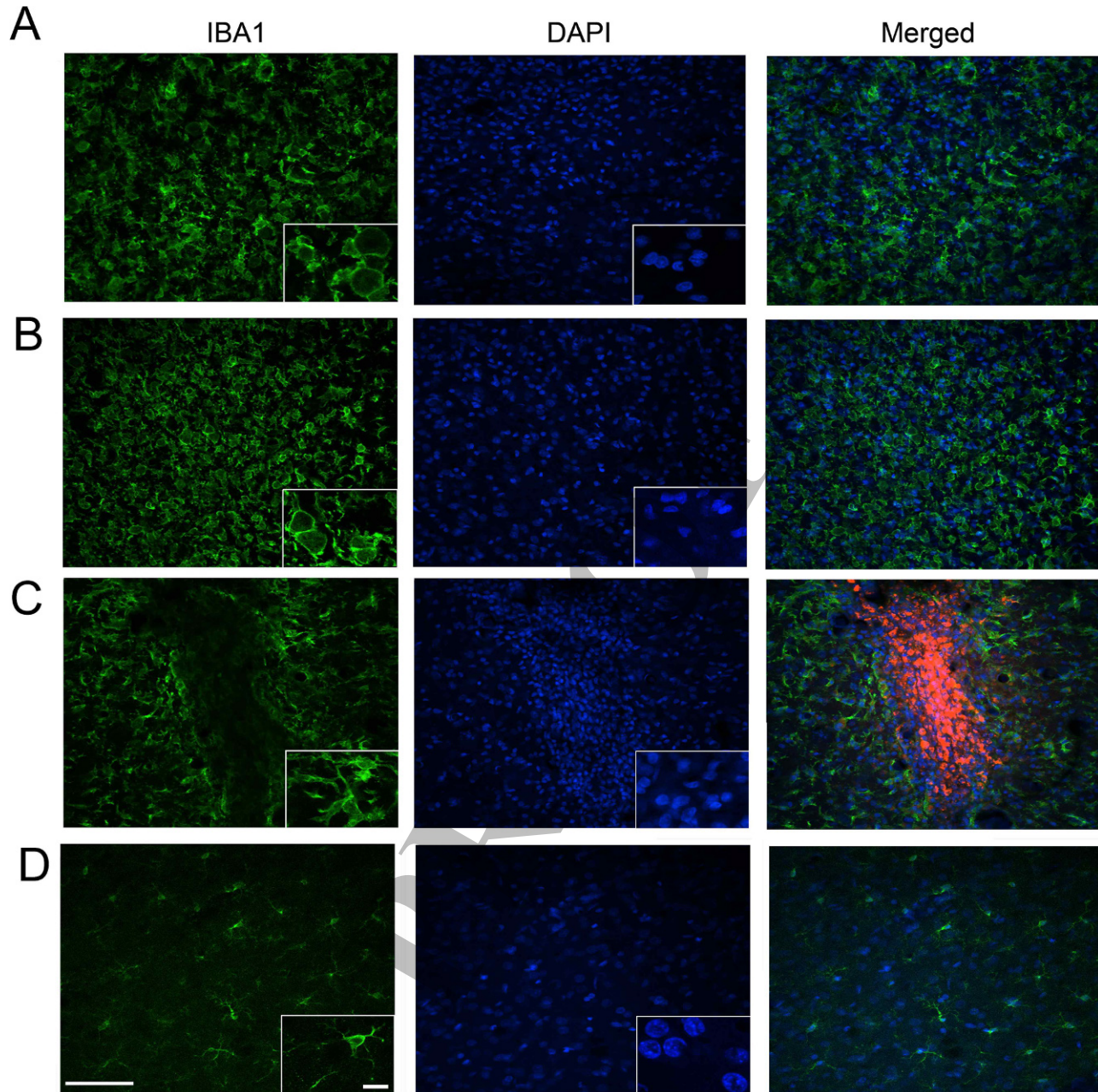
Figure 5. Activation of microglia in the ischemic core area. Enhanced IBA1 immunoreactivity was found in the core of the ischemic cortex (A), compared to the nonlesioned side cortex (D) in an animal receiving vehicle (calibration = 50 ∝m).High-magnification images demonstrate resting microglia exhibiting ramified morphology in the nonlesioned side cortex (D, insert, calibration = 10 ∝m) and deramified or ameboid microglial cells in the lesion core (A, insert), suggesting an activation of microglia. (B) Transplantation of hPDMCs did not alter IBA1 immunoreactivity in regions away from the transplant in core (B vs. A). (C) Partial reduction of IBA1 activation was found near (<300 ∝m) the graft. (C, right panel) hPDMCs were labeled by red CM-DiI fluorescence in the lesioned cortex.

DISCUSSION

In this study, we transplanted hPDMCs into the brains of experimental stroke animals. Stroke rats receiving intracortical hPDMC grafts showed a significant reduction in body asymmetry and neurological symptoms. Using H&E staining and T2WI, we found that transplantation of hPDMCs significantly reduced infarction in stroke rats. Our data support a neuroprotective role of hPDMCs in an animal model of stroke.

hPDMCs were prelabeled with CM-DiI prior to transplantation. We demonstrated that the graft cells survived up to 5 days after transplantation in stroke brain as both
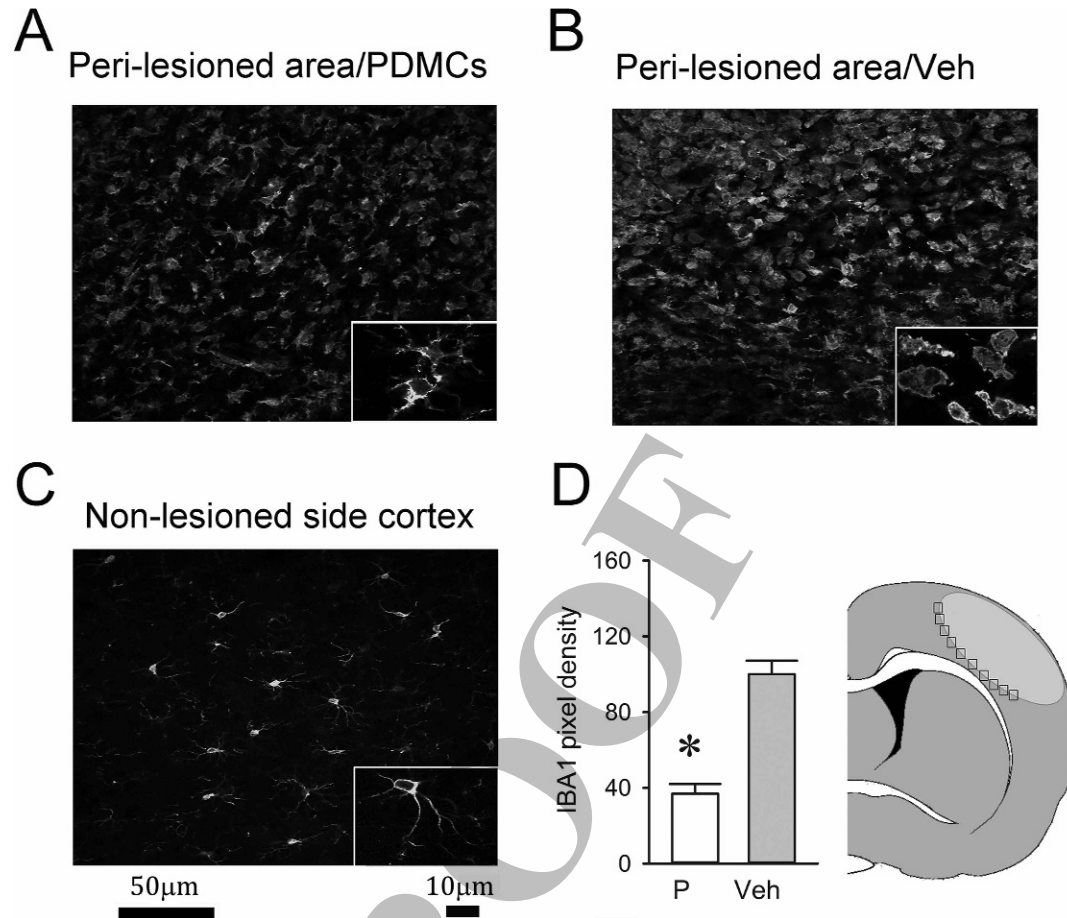
Figure 6. Transplantation of hPDMCs reduced activation of microglia in the perilesioned area. Enhanced IBA-1 immunoreactivity in the perilesioned area (A and B) in the ischemic cortex, compared to the nonlesioned side cortex (C). High-magnification images (inserts) demonstrate deramified or ameboid microglial cells in the perilesioned cortex in animals receiving vehicle (B). Transplantation of hPDMCs reduced the IBA1 immunoreactivity (A vs. B). Ramified microglia were found in the perilesioned area in animals receiving PDMCs (A, insert). Averaged IBA1 optical density in the perilesioned zone was significantly reduced by PDMC transplantation (D). Resting microglia exhibiting ramified morphology were present in the nonlesioned side cortex (C, insert). Calibration, inserts: 10 ∝m.

CM-DiI fluorescence and human-specific marker HuNu were found at the graft sites. Although most of the CM-DiI fluorescent cells were colabeled with HuNu, not all HuNu^{+} cells contained CM-DiI fluorescence. These data suggest that CM-DiI may leak out from hPDMCs during a 5-day period after grafting.

Both peripheral and innate immune responses contribute to the neurodegeneration after stroke. Regulation of peripheral inflammation can modulate brain inflammation after stroke. For example, splenectomy prior to MCAo reduced activated microglia and brain infarction (1). Systemic administration of minocycline reduced morphological activation of microglia in areas adjacent to the infarction in stroke animals (38). Intravenous transplantation of human embryonic neural stem cells (H1 clone) attenuated systemic inflammatory responses and reduced neurological deficits (17). Similar to peripheral inflammation, inflammation of

the brain is also a critical risk factor leading to stroke-mediated damage (12). In this study, we grafted hPDMCs directly into the ischemic brain. A much lower dose of cells were used for intracerebral transplantation, compared to peripheral transplantation reported previously (17). The graft cells were found mainly in the lesioned brain parenchyma after intracerebral transplantation, whereas most cells were found in the spleen with limited numbers in the brain after intravenous grafting (17). We demonstrated that hPDMC grafts reduced IBA1 immunoreactivity and morphological activation of microglia adjacent to the graft and in the perilesioned area. Our data support that hPDMCs induced protection in part, through the suppression of inflammation in stroke brain.

In the nonlesioned brain, naive T-cells are not capable of entering the brain. After injury, activated cluster of differentiation 4-positive (CD4^{+}) and CD8^{+} T-cells pass through

the damaged BBB and populate the lesioned brain area. Both CD4^{+} and CD8^{+} T-cells release the inflammatory mediator IFN- , a key regulator of immune and inflammatory responses. IFN- induces inflammatory chemokines (27) and causes neurodegeneration in the stroke brain (37). These cascade responses are further augmented by ischemic brain injury, which enhances IFN- expression (28) and in turn overexpression of IFN- increases infarcts after MCAo (16). We previously reported that hPDMCs possess strong immunosuppressive properties (8). hPDMCs suppressed CD4^{+} and CD8^{+} T-lymphocytes by increasing regulatory T-lymphocytes (8). Furthermore, PDMCs reduced IL-2-mediated secretion of IFN- when cocultured with NKs. PDMCs also attenuated IL-2/NK-mediated apoptosis by upregulating surface HLA-G, an immunomodulatory molecule, upon exposure to IFN- (21). Taken together, these data suggest that PDMCs may suppress inflammation through modulation of T-cells and the IFN- pathway in the stroke brain.

Similar to the PDMCs, other placental cells also possess protective activity against ischemic brain injury. Intravenously infused placental-derived adherent PDA001 cells reduced lesion volume and terminal deoxynucleotidyl transferase dUTP nick-end labeling (TUNEL), while improving functional outcome in stroke rats (9). Transplantation of dog placental cells produced behavioral recovery and reduced histological deficits in ischemic stroke rats (39). These protective responses have been attributed to the trophic response of placental cells via activation of vascular endothelial growth factor, hepatocyte growth factor (HGF), and brain-derived neurotrophic factor (9), or heat shock protein 27 (HSP27) (39). We recently reported that HGF derived from human mesenchymal stem cells, including hPDMCs, has potent immunomodulatory effects through expansion of diverse populations of immunomodulatory leukocytes, such as myeloid-derived suppressor cells and production of IL-10-producing monocytes (10,33). Similarly, intravenous administration hHSP27 significantly reduced IBA1 expression in the stroke brain (30). It is possible that hPDMCs may also reduce inflammation through these protective factors in stroke animals.

hPDMCs are multilineage stem cells and can be differentiated into neurons, astrocytes, and oligodendrocytes in selective induction media in vitro. Upon induction, PDMCs exhibited outgrowth of processes and the expression of neuron-specific molecules, such as neuron-specific enolase (35). Cytoskeletal rearrangement can also lead to a neural-like phenotype in hPDMCs (33). These neuron-like cells may be useful for regenerating neuronal connections in the lesioned brain. Future studies will determine if hPDMCs can be differentiated into functional neurons in chronic stroke animals.

FA has been used to monitor maturation of white matter (26), myelination in brain development (22), white matter damage (15,34), as well as reorganization of white matter during brain repair (20). We and other laboratories have shown that axonal projections were reorganized, and overall orientation of the axonal projections using DTI was parallel to the lesion boundary with a significant increase in FA values in stroke animals after selective neural reparative treatments (13,15,19,20). In this study, we found a significant reduction in FA ratio in the external capsule of lesioned brains receiving hPDMCs or vehicle on day 4 after MCAo. No difference in FA was seen between these two groups. Our data may suggest that axonal projections to the white matter of the lesioned side is greatly impaired by ischemic brain injury and is not protected by hPDMC grafts.

Acute ischemic brain injury induces cytotoxic edema (cell swelling), inflammation, and cell infiltration lasting from hours to days (25,32). Cytotoxic edema causes a decrease in extracellular volume and results in restriction of microscopic water molecular diffusion (29). An in vitro study demonstrated water ADC decreased both when cells swelled and when cell density increased (2). A similar reduction of the ADC has been reported during inflammation in kidneys (14). In contrast, increasing tissue or extracellular water contributes to an elevation of ADC as seen in the vasogenic edema (29). In the current study, we reported that the rADC was increased in the lesioned cortex receiving hPDMCs, compared to vehicle. Together with the reduction of microglia activation by hPDMCs, our ADC data may imply that hPDMCs reduce inflammation or cytotoxic edema in the stroke brain.

In conclusion, we characterized the immunomodulatory and neuroprotective effects of hPDMCs in an animal model of stroke. The prophylactic use of hPDMCs against stroke has clinical utility to patients prone to ischemic events or with repeated episodes. A comprehensive study is required to examine the poststroke outcomes when hPDMCs are transplanted after brain ischemia. The utility of hPDMCs can extend to other brain diseases. The strong immunomodulatory properties of hPDMCs may encompass other neuroinflammation-related diseases, such as autoimmune encephalitis, traumatic brain injury, and hemorrhagic stroke. Furthermore, as PDMCs are multipotent, grafting of hPDMCs may provide additional neurorepair in the chronic stroke brain.

REFERENCES

1. Ajmo, C. T. Jr.; Vernon, D. O.; Collier, L.; Hall, A. A.; Garbuzova-Davis, S.; Willing, A.; Pennypacker, K. R. The spleen contributes to stroke-induced neurodegeneration. J. Neurosci. Res. 86:2227–2234; 2008.
2. Anderson, A. W.; Xie, J.; Pizzonia, J.; Bronen, R. A.; Spencer, D. D.; Gore, J. C. Effects of cell volume fraction changes on apparent diffusion in human cells. Magn. Reson. Imaging 18:689–695; 2000.

3. Basser, P. J.; Mattiello, J.; LeBihan, D. MR diffusion tensor spectroscopy and imaging. Biophys. J. 66:259–267; 1994.

4. Basser, P. J.; Pierpaoli, C. Microstructural and physiological features of tissues elucidated by quantitative-diffusion-tensor MRI. J. Magn. Reson. B 111:209–219; 1996.

5. Bederson, J. B.; Pitts, L. H.; Tsuji, M.; Nishimura, M. C.; Davis, R. L.; Bartkowski, H. Rat middle cerebral artery occlusion: Evaluation of the model and development of a neurologic examination. Stroke 17:472–476; 1986.

6. Borlongan, C. V.; Hida, H.; Nishino, H. Early assessment of motor dysfunctions aids in successful occlusion of the middle cerebral artery. Neuroreport 9:3615–3621; 1998.

7. Chang, C. F.; Morales, M.; Chou, J.; Chen, H. L.; Hoffer, B. J.; Wang, Y. Bone morphogenetic proteins are involved in fetal kidney tissue transplantation -Induced neuroprotection in stroke rats. Neuropharmacology 43:418–426; 2002.

8. Chang, C. J.; Yen, M. L.; Chen, Y. C.; Chien, C. C.; Huang, H. I.; Bai, C. H.; Yen, B. L. Placenta-derived multipotent cells exhibit immunosuppressive properties that are enhanced in the presence of interferon-gamma. Stem Cells 24:2466–2477; 2006.

9. Chen, J.; Shehadah, A.; Pal, A.; Zacharek, A.; Cui, X.; Cui, Y.; Roberts, C.; Lu, M.; Zeitlin, A.; Hariri, R.; Chopp, M. Neuroprotective effect of human placenta-derived cell treatment of stroke in rats. Cell Transplant. 22:871–879; 2013.

10. Chen, P. M.; Liu, K. J.; Hsu, P. J.; Wei, C. F.; Bai, C. H.; Ho, L. J.; Sytwu, H. K.; Yen, B. L. Induction of immuno-modulatory monocytes by human mesenchymal stem cell-derived hepatocyte growth factor through ERK1/2. J. Leukoc. Biol. 96:295–303; 2014.

11. del Zoppo, G. J. Acute anti-inflammatory approaches to ische-mic stroke. Ann. N. Y. Acad. Sci. 1207:143–148; 2010.

12. del Zoppo, G. J.; Gorelick, P. B. Innate inflammation as the common pathway of risk factors leading to TIAs and stroke. Ann. N. Y. Acad. Sci. 1207:8–10; 2010.

13. Ding, G.; Jiang, Q.; Li, L.; Zhang, L.; Zhang, Z. G.; Ledbetter, K. A.; Panda, S.; Davarani, S. P.; Athiraman, H.; Li, Q.; Ewing, J. R.; Chopp, M. Magnetic resonance imaging investigation of axonal remodeling and angiogenesis after embolic stroke in sildenafil-treated rats. J. Cereb. Blood Flow Metab. 28:1440–1448; 2008.

14. Goyal, A.; Sharma, R.; Bhalla, A. S.; Gamanagatti, S.; Seth, A. Diffusion-weighted MRI in inflammatory renal lesions: All that glitters is not RCC! Eur. Radiol. 23:272–279; 2013.

15. Jiang, Q.; Zhang, Z. G.; Chopp, M. MRI evaluation of white matter recovery after brain injury. Stroke 41:S112–S113; 2010.

16. Lambertsen, K. L.; Gregersen, R.; Meldgaard, M.; Clausen, B. H.; Heibol, E. K.; Ladeby, R.; Knudsen, J.; Frandsen, A.; Owens, T.; Finsen, B. A role for interferon-gamma in focal cerebral ischemia in mice. J. Neuropathol. Exp. Neurol. 63:942–955; 2004.

17. Lee, S. T.; Chu, K.; Jung, K. H.; Kim, S. J.; Kim, D. H.; Kang, K. M.; Hong, N. H.; Kim, J. H.; Ban, J. J.; Park, H. K.; Kim, S. U.; Park, C. G.; Lee, S. K.; Kim, M.; Roh, J. K. Anti-inflammatory mechanism of intravascular neural stem cell transplantation in haemorrhagic stroke. Brain 131:616–629; 2008.

18. Lee, Y.; Lee, S. R.; Choi, S. S.; Yeo, H. G.; Chang, K. T.; Lee, H. J. Therapeutically targeting neuroinflammation and microglia after acute ischemic stroke. Biomed. Res. Int. 2014:297241; 2014.

19. Li, L.; Jiang, Q.; Ding, G.; Zhang, L.; Zhang, Z. G.; Li, Q.; Panda, S.; Kapke, A.; Lu, M.; Ewing, J. R.; Chopp, M. MRI identification of white matter reorganization enhanced by erythropoietin treatment in a rat model of focal ischemia. Stroke 40:936–941; 2009.

20. Liu, H. S.; Shen, H.; Harvey, B. K.; Castillo, P.; Lu, H.; Yang, Y.; Wang, Y. Post-treatment with amphetamine enhances reinnervation of the ipsilateral side cortex in stroke rats. Neuroimage. 56:280–289; 2011.

21. Liu, K. J.; Wang, C. J.; Chang, C. J.; Hu, H. I.; Hsu, P. J.; Wu, Y. C.; Bai, C. H.; Sytwu, H. K.; Yen, B. L. Surface expression of HLA-G is involved in mediating immunomod-ulatory effects of placenta-derived multipotent cells (PDMCs) towards natural killer lymphocytes. Cell Transplant. 20:1721–1730; 2011.

22. Lobel, U.; Sedlacik, J.; Gullmar, D.; Kaiser, W. A.; Reichenbach, J. R.; Mentzel, H. J. Diffusion tensor imaging: The normal evolution of ADC, RA, FA, and eigenvalues studied in multiple anatomical regions of the brain. Neuro-radiology 51:253–263; 2009.

23. Luo, Y.; Kuo, C. C.; Shen, H.; Chou, J.; Greig, N. H.; Hoffer, B. J.; Wang, Y. Delayed treatment with a p53 inhibi-tor enhances recovery in stroke brain. Ann. Neurol. 65:520–530; 2009.

24. Luo, Y.; Shen, H.; Liu, H. S.; Yu, S. J.; Reiner, D. J.; Harvey, B. K.; Hoffer, B. J.; Yang, Y.; Wang, Y. CART peptide induces neuroregeneration in stroke rats. J. Cereb. Blood Flow Metab. 33:300–310; 2013.

25. Morioka, T.; Kalehua, A. N.; Streit, W. J. Characterization of microglial reaction after middle cerebral artery occlusion in rat brain. J. Comp. Neurol. 327:123–132; 1993.

26. Provenzale, J. M.; Liang, L.; DeLong, D.; White, L. E. Dif-fusion tensor imaging assessment of brain white matter matu-ration during the first postnatal year. AJR Am. J. Roentgenol. 189:476–486; 2007.

27. Seifert, H. A.; Collier, L. A.; Chapman, C. B.; Benkovic, S. A.; Willing, A. E.; Pennypacker, K. R. Pro-inflammatory inter-feron gamma signaling is directly associated with stroke induced neurodegeneration. J. Neuroimmune Pharmacol. 9:679–689; 2014.

28. Seifert, H. A.; Leonardo, C. C.; Hall, A. A.; Rowe, D. D.; Collier, L. A.; Benkovic, S. A.; Willing, A. E.; Pennypacker, K. R. The spleen contributes to stroke induced neuro degen-eration through interferon gamma signaling. Metab. Brain Dis. 27:131–141; 2012.

29. Sotak, C. H. The role of diffusion tensor imaging in the evaluation of ischemic brain injury - A review. NMR Biomed. 15:561–569; 2002.

30. Teramoto, S.; Shimura, H.; Tanaka, R.; Shimada, Y.; Miyamoto, N.; Arai, H.; Urabe, T.; Hattori, N. Human-derived physiological heat shock protein 27 complex protects brain after focal cerebral ischemia in mice. PLoS One 8:e66001; 2013.

31. Ting, C. H.; Ho, P. J.; Yen, B. L. Age-related decreases of serum-response factor levels in human mesenchymal stem cells are involved in skeletal muscle differentiation and engraftment capacity. Stem Cells Dev. 23:1206–1216; 2014.

32. Tobin, M. K.; Bonds, J. A.; Minshall, R. D.; Pelligrino, D. A.; Testai, F. D.; Lazarov, O. Neurogenesis and inflamma-tion after ischemic stroke: What is known and where we go from here. J. Cereb. Blood Flow Metab. 34:1573–1584; 2014.

33. Wang, C. H.; Wu, C. C.; Hsu, S. H.; Liou, J. Y.; Li, Y. W.; Wu, K. K.; Lai, Y. K.; Yen, B. L. The role of RhoA kinase inhibition in human placenta-derived multipotent cells on neural phenotype and cell survival. Biomaterials 34:3223–3230; 2013.

34. Watanabe, T.; Honda, Y.; Fujii, Y.; Koyama, M.; Matsuzawa, H.; Tanaka, R. Three-dimensional anisotropy contrast magnetic resonance axonography to predict the prognosis for motor function in patients suffering from stroke. J. Neurosurg. 94:955–960; 2001.

35. Yen, B. L.; Chien, C. C.; Chen, Y. C.; Chen, J. T.; Huang, J. S.; Lee, F. K.; Huang, H. I. Placenta-derived multipotent cells differentiate into neuronal and glial cells in vitro. Tissue Eng. Part A 14:9–17; 2008.

36. Yen, B. L.; Huang, H. I.; Chien, C. C.; Jui, H. Y.; Ko, B. S.; Yao, M.; Shun, C. T.; Yen, M. L.; Lee, M. C.; Chen, Y. C. Isolation of multipotent cells from human term placenta. Stem Cells 23:3–9; 2005.

37. Yilmaz, G.; Arumugam, T. V.; Stokes, K. Y.; Granger, D. N. Role of T lymphocytes and interferon-gamma in ischemic stroke. Circulation 113:2105–2112; 2006.

38. Yrjanheikki, J.; Tikka, T.; Keinanen, R.; Goldsteins, G.; Chan, P. H.; Koistinaho, J. A tetracycline derivative, minocycline, reduces inflammation and protects against focal cerebral ischemia with a wide therapeutic window. Proc. Natl. Acad. Sci. USA 96:13496–13500; 1999.

39. Yu, S.; Tajiri, N.; Franzese, N.; Franzblau, M.; Bae, E.; Platt, S.; Kaneko, Y.; Borlongan, C. V. Stem cell-like dog placenta cells afford neuroprotection against ischemic stroke model via heat shock protein upregulation. PLoS One 8: e76329; 2013.

40. Yu, S. J.; Airavaara, M.; Shen, H.; Chou, J.; Harvey, B. K.; Wang, Y. Suppression of endogenous PPAR increases vulnerability to methamphetamine-induced injury in mouse nigrostriatal dopaminergic pathway. Psychopharmacology 221:479–492; 2012.